Journal of Magnetism and Magnetic Materials 409 (2016) 39–44

Contents lists available at ScienceDirect

Journal of Magnetism and Magnetic Materials

journal homepage: www.elsevier.com/locate/jmmm

Corrosion resistance of sintered NdFeB coated with SiC/Al bilayer thin films by magnetron sputtering

Yiqin Huang [a], Heqin Li [a,*], Min Zuo [a], Lei Tao [a], Wei Wang [a], Jing Zhang [a,b], Qiong Tang [a,b], Peiwen Bai [a]

[a] School of Materials Science and Engineering, Hefei University of Technology, Hefei 230009, China
[b] School of Electronic Science and Applied Physics, Hefei University of Technology, Hefei 230009, China

ARTICLE INFO

Article history:
Received 7 October 2015
Received in revised form
1 February 2016
Accepted 4 February 2016

Keywords:
NdFeB magnet
SiC/Al bilayer films
Magnetron sputtering
Corrosion resistance

ABSTRACT

The poor corrosion resistance of sintered NdFeB imposes a great challenge in industrial applications. In this work, the SiC/Al bilayer thin films with the thickness of 510 nm were deposited on sintered NdFeB by magnetron sputtering to improve the corrosion resistance. A 100 nm Al buffer film was used to reduce the internal stress between SiC and NdFeB and improve the surface roughness of the SiC thin film. The morphologies and structures of SiC/Al bilayer thin films and SiC monolayer film were investigated with FESEM, AFM and X-ray diffraction. The corrosion behaviors of sintered NdFeB coated with SiC monolayer film and SiC/Al bilayer thin films were analyzed by polarization curves. The magnetic properties were measured with an ultra-high coercivity permanent magnet pulse tester. The results show that the surface of SiC/Al bilayer thin films is more compact and uniform than that of SiC monolayer film. The corrosion current densities of SiC/Al bilayer films coated on NdFeB in acid, alkali and salt solutions are much lower than that of SiC monolayer film. The SiC/Al bilayer thin films have little influence to the magnetic properties of NdFeB.

1. Introduction

NdFeB permanent magnets have been widely used in many fields due to their high remanence, coercive force and maximum magnetic energy product [1–3]. However, the chemical stability of NdFeB is poor because of its multiphase microstructures which consist of $Nd_2Fe_{14}B$ main phase, Nd-rich and B-rich phases [4–5]. NdFeB is prone to oxidize under the daily use, and serious electrochemical corrosion will happen under hot and humid atmospheres. The corrosion problems of NdFeB have become the bottleneck of limiting applications [6].

There are many attempts to improve the anti-corrosion quality of sintered NdFeB permanent magnets, such as adding alloy elements which is at the expense of magnetic properties [7], surface electroplating and chemical plating in industry [8]. However, electroplating is often associated with the environment problems and it will deteriorate NdFeB magnetic performance at certain extent [9]. As one of the environmental friendly technologies, physical vapor deposition technology (PVD) has advantages of good adhesive force between film and substrate, higher film quality and less influence on its magnetic performance. PVD is increasingly applied in NdFeB surface corrosion resistance compared with electroplating [10–14]. In recent years, Ti/TiN, Al/AlN and Al/Al_2O_3 coatings have been deposited on sintered NdFeB by PVD [15–17]. However, there has been lack of information about SiC/Al bilayer films prepared on NdFeB by magnetron sputtering. Al coating possesses the outstanding ductility, and Al (0.406 nm) has the similar lattice constant with SiC (0.436 nm). Furthermore, there are the interfacial reaction and metallurgy bonding between Al coating and NdFeB substrate [16], so Al can improve the adhesive strength of the SiC film with the NdFeB substrate. SiC has the good resistance to high temperature oxidation and corrosion, high thermal conductivity, good wear-resisting performance and strong radiation resistance [18–19]. The SiC/Al-coated on NdFeB is a promising way to improve the corrosion resistance. This paper has studied SiC/Al bilayer and SiC monolayer thin films deposited on sintered NdFeB magnets by magnetron sputtering.

2. Experimental details

2.1. The preparation of thin films

The thin films were prepared with FJL560B1 type ultrahigh vacuum magnetron sputtering equipment (SKY Technology Development Co., Ltd. Chinese Academy of Sciences). The whole

* Corresponding author.
E-mail address: lhqjs@hfut.edu.cn (H. Li).

http://dx.doi.org/10.1016/j.jmmm.2016.02.006
0304-8853/

Table 1
NdFeB magnet composition.

NdFeB (42M)	Pr, Nd	B	Dy	Fe	Others
wt%	30.33	1.02	1.81	65.8	1.04

Table 2
Specific deposition parameters of different thin films.

Coating	Layer	Power (W)	Work pressure (Pa)	Deposition time (min)	Controlled thickness (nm)	Ar flow rate (sccm)
Al single layer		50	0.5	154	510	40
SiC single layer		150	0.5	112	510	60
SiC/Al layers	Al	50	0.5	30	100	40
	SiC	150	0.5	90	410	60

sputtering process was at room temperature. The sintered SiC (purity 99.5%) and metal Al (purity 99.99%) were used for targets. The sintered NdFeB specimen (No. 42M) which compositions were listed in Table 1, with a size of 12.60 mm × 7.60 mm × 0.90 mm were ground and polished to a mirror surface and then ultrasonically cleaned under acetone followed by alcohol before coating. The base pressure of sputtering chamber was 1.0×10^{-4} Pa and the deposition was carried out under Ar atmosphere. We also pre-sputtered the Al and SiC targets before deposition.

Al and SiC films were sputtered by DC and RF magnetron sputtering in sequence, which realized the growth of Al and SiC thin films in turn. For comparison, pure Al and SiC single thin films which have the same thickness with SiC/Al bilayer thin films were also prepared. The specific deposition parameters were listed in Table 2.

2.2. The structures and performances of the thin films

The crystal structures of the films were measured by an X-ray diffraction (XRD, D/Max2500V, Rigaku) with Cu Kα radiation. The surface and cross-sectional morphologies of the SiC/Al thin films were measured with an atomic force microscope (AFM, CSPM5500A, Chemistry primitive nano instrument Co., Ltd. Chinese Academy of Sciences) and a field emission scanning electron microscope (FESEM, SU8020, Hitachi) respectively. The thickness of Al film and SiC film were measured with FESEM. The magnetic properties (remanence, coercivity and maximum energy product) of NdFeB coated with SiC/Al were measured by an ultra-high coercivity permanent magnet pulse tester (PFM12.cn, Hirst Magnetic Instruments Ltd, Britain).

The electrochemical corrosion behaviors of the specimens were evaluated by potentiodynamic polarization in 0.62 mol/L NaCl, 6.25 mol/L NaOH and 0.10 mol/L H_2SO_4 solutions having PH of 7, 14, 1 respectively by extensive PH indicator paper at 25 ± 3 °C, using a CHI650D electrochemical analyzer (Shanghai Chenhua, China). A conventional three-electrode cell was used with the Ag/AgCl as the reference electrode and a platinum sheet as the counter electrode. The exposed surface area of the working electrodes was 0.94 cm^2. The electrolyte was aerated and the specimens as working electrode were kept in the solutions for 1 h before the potentiodynamic polarization test to obtain the stable potential, and the scanning speed was 2 mv/s with the applied potential varied from −1.4 V to −0.2 V. We fixed the wire at the sample's backside and then lacquered the backside and all four sides so that we could only test the surface corrosion resistant rather than the sides and backside of samples.

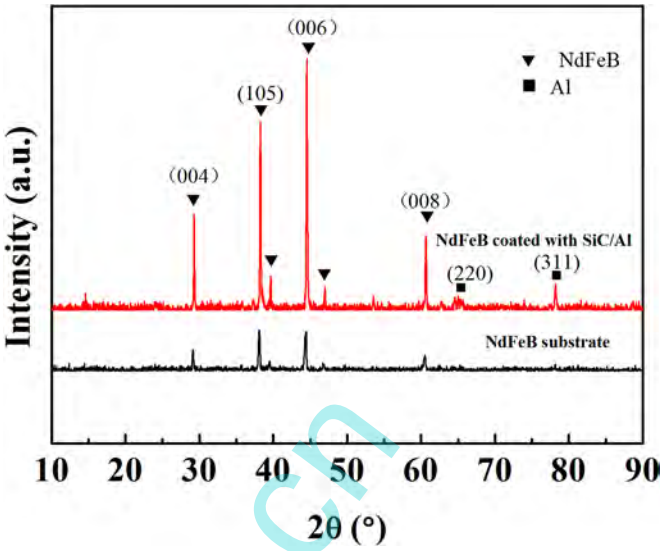

Fig. 1. XRD patterns of NdFeB substrate and NdFeB coated with SiC/Al.

3. Results and discussion

3.1. Structures of thin films

Fig. 1 shows the XRD patterns of the NdFeB substrate and SiC/Al coated on NdFeB. There are four major diffraction peaks of $Nd_2Fe_{14}B$ (004), (105), (006), (008) and two diffractive peaks of Al (220), (311), which indicates that NdFeB and Al film are crystalline. However, SiC broad diffraction peak is unclear because the strong diffraction peak of NdFeB covers up it and the film thickness of SiC is too thin to be diffracted. Furthermore, some extra small diffractive peaks of $Nd_2Fe_{14}B$ are also observed and the intensity of main diffractive peaks is strengthened after sputtering SiC/Al films, because the bombardments of sputtering particles to the NdFeB substrate will provide an extra crystallizing energy for $Nd_2Fe_{14}B$.

3.2. Morphologies of thin films

Fig. 2 shows AFM (scanning range is 5 × 5 μm^2) micrographs of the SiC monolayer film and SiC/Al bilayer films. The particle size of SiC monolayer film is inhomogeneous and rough in Fig. 2a, while SiC/Al bilayer films exhibit a flat surface, and small uniform particles in Fig. 2b. Table 3 shows the average particle diameters and roughness of SiC and SiC/Al thin films. The average particle diameter and roughness parameters of SiC monolayer film are 212 nm and 6.17 nm respectively, while the corresponding parameters of SiC/Al bilayer films are 193 nm and 3.82 nm respectively. This means the Al buffer layer acts on the smoothing surface of the SiC thin film.

SiC monolayer film has larger particles and roughness than that of SiC/Al bilayer films, and there are some micropores on its surface from AFM observation. The particles of SiC/Al thin films are smaller and denser, and the film surface is smoother and has little apparent defects, which is related to three aspects. First, there are some pores on NdFeB substrates coming from powder metallurgy process, thus SiC monolayer film cannot completely cover these slots. Second, there are the interfacial diffusion reaction of Al, Fe and Nd and metallurgy bonding between the Al coating and NdFeB substrate [17], which means the Al coating has combined well with NdFeB substrate. Furthermore, Al (0.406 nm) has the similar

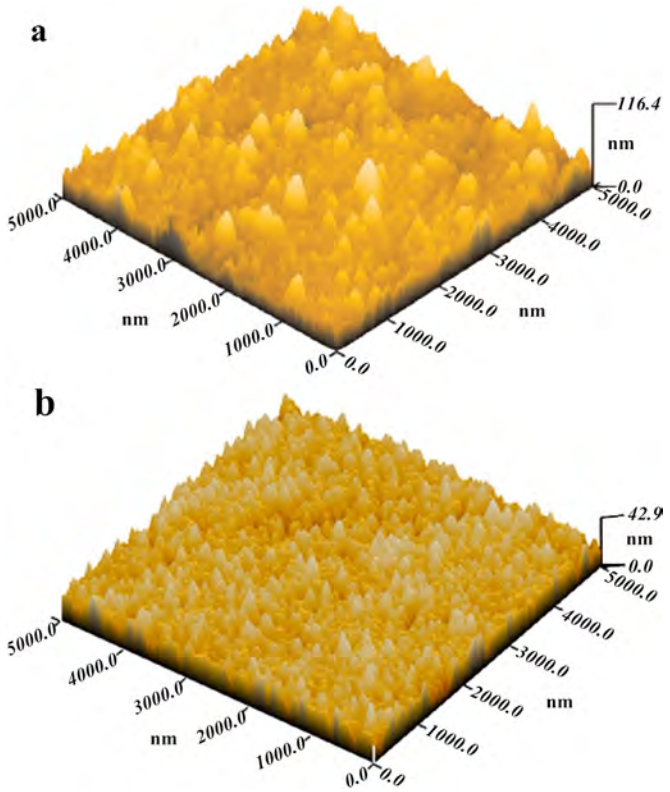

Fig. 2. AFM morphologies (a) SiC monolayer film and (b) SiC/Al bilayer films.

Table 3
The AFM data of SiC and SiC/Al thin films coated on NdFeB.

Specimens	The average particle diameter (nm)	The average roughness (nm)
SiC/NdFeB	212	6.17
SiC/Al/NdFeB	193	3.82

lattice constant with SiC (0.436 nm), they can match well in boundary. Thus, Al buffer layer is a good imbedded layer which can effectively reduce the internal stress caused by mismatch between SiC and NdFeB and improve the surface roughness of SiC coated on NdFeB.

Fig. 3 shows FESEM micrographs of the surface and the cross section of SiC/Al bilayer films coated on NdFeB. Fig. 3a presents a nano-crystal surface of SiC/Al bilayer films, and Fig. 3b is a cross-sectional SEM image of SiC/Al films coated on NdFeB, in which SiC film exhibits a slight columnar structure, and the thicknesses of Al and SiC thin films are 100 nm and 410 nm respectively.

3.3. Corrosion resistance of films

Fig.4 shows the potentiodynamic polarization curves for NdFeB substrate, and the same thick Al, SiC and SiC/Al-coated on NdFeB in 0.62 mol/L NaCl, 6.25 mol/L NaOH and 0.10 mol/L H_2SO_4 solutions respectively. The corrosion potential E_{corr} and current density I_{corr} calculated by Tafel extrapolation are listed in Table 4. According to Faraday law, during the electrochemical corrosion process, the relationship between corrosion rate and corrosion current density is as follows [20]:

$$\nu = \frac{MI_{corr}}{nF}$$

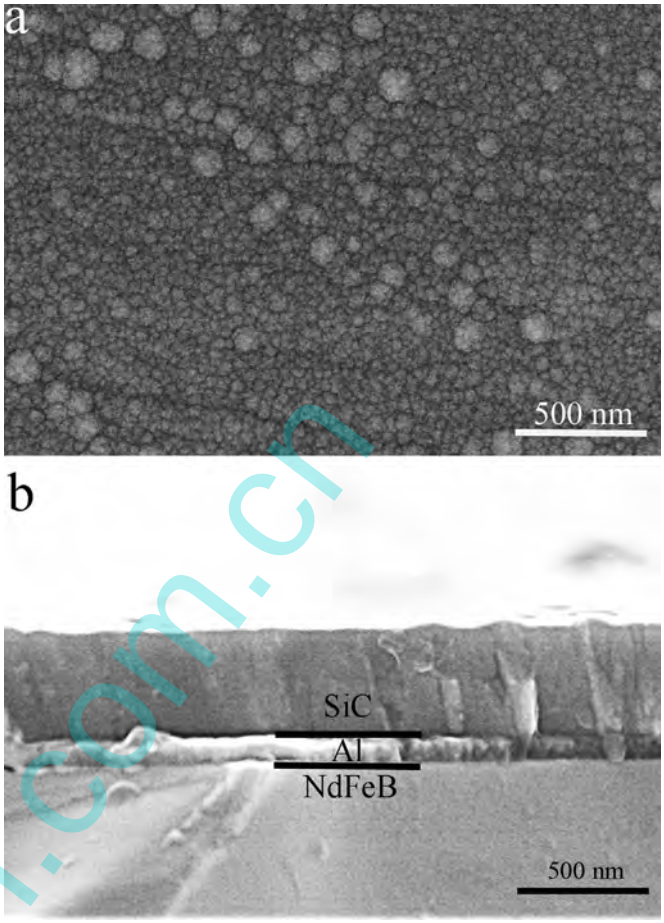

Fig. 3. FESEM (a) surface and (b) cross-section micrographs of the SiC/Al bilayer films coated on NdFeB.

where ν is corrosion rate, M is the atomic mass of corrosion metal, n is the chemical valence state and F is Faraday's constant. It can be seen that the corrosion rate is directly proportional to the corrosion current density for a certain material.

A shift of the whole polarization curves towards the region of lower current density and the higher potential indicates the obvious improvements of the corrosion resistances for the coated NdFeB. E_{corr} and I_{corr} (vs. Ag/AgCl) of bare NdFeB, Al-coated, SiC-coated and SiC/Al-coated on NdFeB specimens are -0.697 V and 1.545×10^{-5} A/cm^2, -0.823 V and 3.764×10^{-6} A/cm^2, -0.528 V and 1.474×10^{-6} A/cm^2, -0.261 V and 9.078×10^{-9} A/cm^2 in 0.62 mol/L NaCl solution respectively. I_{corr} order is NdFeB > Al-coated > SiC-coated > SiC/Al-coated, and SiC/Al bilayer films have about two orders of magnitude lower than that of SiC monolayer film, which reveals that the corrosion resistance of SiC monolayer film is improved due to the intercalation of Al layer. Furthermore, the surface of uncoated NdFeB is full of yellow rust quickly (Fig. 5a), while the SiC-coated surface is distributed little gray rust (Fig. 5b) and the SiC/Al-coated surface is still shining and almost intact (Fig. 5c) in 0.62 mol/L NaCl solution. This corrosion morphology is consistent with the potentiodynamic polarization results in 0.62 mol/L NaCl solution.

The corrosion resistance of SiC/Al/NdFeB is superior to that of SiC/NdFeB, which is closely related to the coating structure. First, there are many micropores on the sintered NdFeB substrate, meanwhile SiC monolayer film presents a cross sectional columnar structure in Fig. 3b and surface holes in Fig. 2a, which may be prone to the corrosive media penetration and brought about the pitting corrosion. However, Al buffer layer can avoid the direct

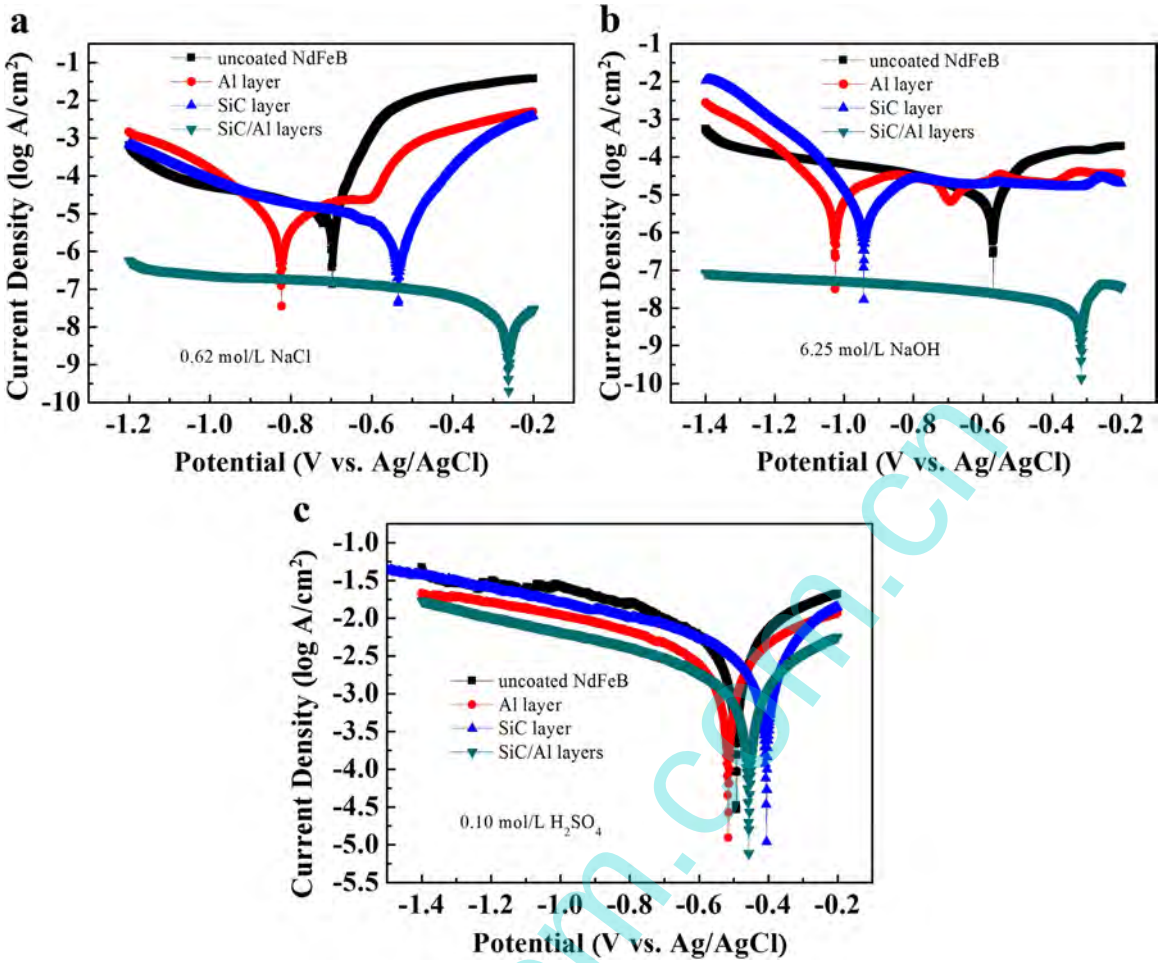

Fig. 4. Potentiodynamic polarization curves of the NdFeB substrate, Al, SiC and SiC/Al-coated on NdFeB in (a) 0.62 mol/L NaCl, (b) 6.25 mol/L NaOH and (c) 0.10 mol/L H_2SO_4 solutions (E_{corr}/V, I_{corr}/(Acm^{-2})).

Table 4
Polarization data of Al, SiC and SiC/Al-coated on NdFeB.

Solutions	Specimens							
	Bare NdFeB		Al/NdFeB		SiC/NdFeB		SiC/Al/NdFeB	
	E_{corr}(V)	I_{corr}(A/cm^2)	E_{corr}(V)	I_{corr}(A/cm^2)	E_{corr}(V)	I_{corr}(A/cm^2)	E_{corr}(V)	I_{corr}(A/cm^2)
NaCl	−0.697	1.545×10^{-5}	−0.823	3.764×10^{-6}	−0.528	1.474×10^{-6}	−0.261	9.078×10^{-9}
NaOH	−0.570	1.304×10^{-5}	−1.026	1.012×10^{-5}	−0.944	4.049×10^{-6}	−0.316	2.003×10^{-9}
H_2SO_4	−0.492	2.713×10^{-3}	−0.516	1.912×10^{-3}	−0.406	1.733×10^{-3}	−0.457	5.742×10^{-4}

contact between the NdFeB substrate and column SiC film and inhibit the electrolytic permeation by column channels. In addition, the additional Al buffer layer can decrease the lattice mismatch between SiC film and NdFeB substrate. This will decrease the surface roughness of the SiC thin film and improve the adhesion of SiC film with NdFeB substrate.

By comparing the polarization curves (Fig. 4a) of NdFeB with Al/NdFeB, the bare sintered NdFeB exhibits an actively dissolving behavior in the electrolyte. However, the anodic branch of the Al film coated on NdFeB exhibits three stages. First, the corrosion current density increases slowly with the increasing corrosion potential from −0.80 V to −0.60 V, and this slow anodic soluble corrosion behavior of Al film comes from the formed passive film on Al film in the electrolyte [21], which can partly prevent the Al coating from corrosion reaction and will benefit of the NdFeB protection. At second stage, the corrosion current density increases rapidly with the corrosion potential increasing from −0.60 V to −0.48 V, which means the actively dissolving of Al passive film and accompanying some micro-pores occurrence on Al film. At final stage, the polarization curve variation of Al film coated on NdFeB is similar to bare NdFeB as corrosion potential is more than −0.48 V, which implies that the dissolution rate of passive film is slightly more than the its growing rate. There are some micro-pores on the passive film at second stage corrosion, which makes the fresh Al surface expose to corrosion solution and accelerate the dissolution of Al film. Al single film will lose the protective effects on NdFeB, once its surface passive film is damaged.

In addition, E_{corr} order is Al-coated (−0.823 V) < bare NdFeB (−0.697 V) < SiC-coated (−0.528 V) < SiC/Al-coated (−0.261 V) in 0.62 mol/L NaCl solution respectively. Al layer mainly acts on the sacrificial protection for NdFeB while SiC layer is a surface protective coating as they contact each other in electrolyte.

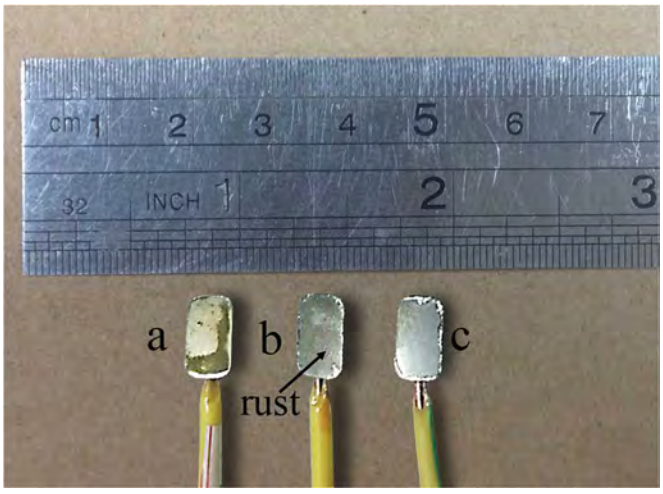

Fig. 5. The photos of (a) bare NdFeB (b) SiC/NdFeB (c) SiC/Al/NdFeB after potentiodynamic polarization test in 0.62 mol/L NaCl solution. (For interpretation of the references to color in this figure, the reader is referred to the web version of this article.)

Table 5
Magnetic properties of the coated SiC/Al bilayer films and bare NdFeB specimens.

Specimens	Magnetic properties		
	Remanence, B_r /kG	Coercive force, H_{cj}/kOe	Maximum energy product, $(BH)_{max}$/MGOe
NdFeB	13.21	15.02	40.13
SiC/Al/NdFeB	12.86	15.29	38.89

Among three kinds of solutions, the SiC/Al bilayer films exhibit the best corrosion resistance in 6.25 mol/L NaOH solution, and the worst corrosion resistance in 0.10 mol/L H_2SO_4 solution, because I_{corr} of the SiC/Al coated on NdFeB in 0.10 mol/L H_2SO_4 solution is 5.742×10^{-4} (Table 5), which is much more than that in NaCl and NaOH solutions. Furthermore, there is the selectively intergranular corrosion of NdFeB in H_2SO_4 solution based on Ref. [22], once the acid solution penetrates into the NdFeB substrate through the surface pores, the NdFeB coated with SiC/Al will bubble violently as our experimental observation.

3.4. Magnetic properties

Table 5 shows the magnetic properties of SiC/Al/NdFeB and bare NdFeB specimens. The remanence (B_r) value and maximum magnetic energy product $(BH)_{max}$ of SiC/Al/NdFeB have slightly decreased, however its coercive force (H_{cj}) has increased distinctly comparing with the bare NdFeB specimen. The magnetic properties of the SiC/Al/NdFeB may be ascribed to two reasons. On the one hand, the plasma bombarding NdFeB substrate surface during coating may pin up the magnetic domains and this contributes to the enhancement of the H_{cj}. On the other hand, the diffractive peak strength of NdFeB coated SiC/Al bilayer films is higher than that of bare NdFeB according to XRD patterns in Fig. 1, which indicated that the crystallinity of NdFeB is enhanced after coating and more grain boundaries can impede the magnetic domain to rotate during magnetizing and demagnetizing, so the coercive force of coated NdFeB increases [23–24]. Meanwhile, there are some the lattice distortion in NdFeB coated SiC/Al due to interface atomic mismatch. The magnetic permeability of NdFeB close to mismatch region decreases and the magnetic flux density also reduces, which lead to maximum magnetic energy product $(BH)_{max}$ decrease slightly.

4. Conclusions

(1) The SiC/Al bilayer films are successfully prepared on the sintered NdFeB substrates by magnetron sputtering. The XRD patterns show that the prepared Al film is crystalline and the diffractive peak of SiC is unclear.
(2) The Al buffer layer can effectively reduce the internal stress between SiC and NdFeB and improve the surface roughness of SiC coated on NdFeB. The particles of SiC/Al thin films are smaller and denser and the film surface is smoother and has little apparent defects than those of SiC monolayer film.
(3) The corrosion resistance of NdFeB coated with SiC/Al bilayer films is better than that coated with SiC monolayer film in three kinds of solutions, because Al buffer layer reduces the structure defect of SiC monolayer and acts on the sacrifice layer for NdFeB substrate. SiC/Al/NdFeB expresses the worst corrosion resistance in the 0.10 mol/L H_2SO_4 solution.
(4) The coated SiC/Al bilayer films do not deteriorate the magnetic properties of NdFeB substrates.

Acknowledgments

The authors gratefully acknowledge the support of the "Strategic Priority Research Program" of the Chinese Academy of Science (Grant no. XDA03040000), and the Earth-Panda Advance Magnetic Material Co., Ltd Fund (Grant no.13-332).

References

[1] J.W. Zheng, M. Lin, Q.P. Xia, A preparation method and effects of Al–Cr coating on NdFeB sintered magnets, J. Magn. Magn. Mater. 324 (2012) 3966–3969.
[2] J.W. Zheng, H.B. Chen, L. Qiao, M. Lin, L.Q. Jiang, S.L. Che, Y.W. Hu, Double coating protection of Nd–Fe–B magnets: Intergranular phosphating treatment and copper plating, J. Magn. Magn. Mater. 371 (2014) 1–4.
[3] T.T. Xie, S.D. Mao, C. Yu, S.J. Wang, Z.L. Song, Structure, corrosion, and hardness properties of Ti/Al multilayers coated on NdFeB by magnetron sputtering, Vacuum 86 (2012) 1583–1588.
[4] L.A. Dobrzanski, M. Drak, J. Trzaska, Corrosion resistance of the polymer matrix hard magnetic composite materials Nd–Fe–B, J. Mater. Process. Technol. 164 (2005) 795–804.
[5] S.M. Tamborim Takeuchi, D.S. Azambuja, A.M. Saliba-Silva, I. Costa, Corrosion protection of NdFeB magnets by phosphating with tungstate incorporation, Surf. Coat. Technol. 200 (2006) 6826–6831.
[6] Q. Li, X.K. Yang, L. Zhang, J.P. Wang, B. Chen, Corrosion resistance and mechanical properties of pulse electrodeposited Ni–TiO_2 composite coating for sintered NdFeB magnet, J. Alloy. Compd. 482 (2009) 339–344.
[7] S.D. Mao, H.X. Yang, J.L. Li, F. Huang, Z.L. Song, Corrosion properties of aluminium coatings deposited on sintered NdFeB by ion-beam-assisted deposition, Appl. Surf. Sci. 257 (2011) 5581–5585.
[8] S.X. Yu, L. Chen, Preparation Technology and Performances of Zn-Cr Coating on Sintered NdFeB Permanent Magnet, J. Rare Earth 24 (2006) 223–226.
[9] S.D. Mao, H.X. Yang, Z.L. Song, J.L. Li, H.G. Ying, K.F. Sun, Corrosion behaviour of sintered NdFeB deposited with an aluminium coating, Corros. Sci. 53 (2011) 1887–1894.
[10] L. Tao, H.Q. Li, J. Shen, K. Qiao, W. Wang, C. Zhou, J. Zhang, Q. Tang, Corrosion resistance of the NdFeB coated with AlN/SiC bilayer thin films by magnetron sputtering under different environments, J. Magn. Magn. Mater. 375 (2015) 124–128.
[11] S.D. Mao, T.T. Xie, B.Z. Zheng, F. Huang, Z.L. Song, Y.X. Li, Structures and properties of sintered NdFeB coated with IBAD-Al/Al_2O_3 multilayers, Surf. Coat. Technol. 207 (2012) 149–154.
[12] N.C. Ku, C.D. Qin, D.H.L. Ng, Enhanced corrosion resistance of NdFeB type permanent magnet coated by a dual layer of either Ti/Al or Ni/Al intermetallics, IEEE. Trans. Magn. 33 (1997) 3913–3915.
[13] N.C. Ku, C.D. Qin, C.C. Yu, D.H.L. Ng, Corrosion resistance of NdFeB magnets coated by Al, IEEE. Trans. Magn. 32 (1996) 4407–4409.
[14] C.D. Qin, A.S.K. Li, D.H.L. Ng, The protective coatings of NdFeB magnets by Al and Al(Fe), J. Appl. Phys. 79 (1996) 4854–4856.
[15] Y.Y. Cheng, X.L. Pang, K.W. Gao, H.S. Yang, A.A. Volinsky, Corrosion resistance and friction of sintered NdFeB coated with Ti/TiN multilayers, Thin Solid Films 550 (2014) 428–434.
[16] J.L. Li, S.D. Mao, K.F. Sun, X.M. Li, Z.L. Song, AlN/Al dual protective coatings on NdFeB by DC magnetron sputtering, J. Magn. Magn. Mater. 321 (2009)

3799–3803.
[17] S.D. Mao, H.X. Yang, F. Huang, T.T. Xie, Z.L. Song, Corrosion behaviour of sintered NdFeB coated with Al/Al_2O_3 multilayers by magnetron sputtering, Appl. Surf. Sci. 257 (2011) 3980–3984.
[18] S. Kerdiles, R. Rizk, A. Pperez-rodrigufz, B. Garrido, O. González-Varona, L. Calvo-Barrio, J.R. Morante, Magnetron sputtering synthesis of silicon carbon films: structural and optical characterization, J. Solid State Electrochem. 42 (1998) 2315–2320.
[19] Z.Y. Li, L.L. Yang, D.T. Ge, Y.B. Ding, L. Pan, J.P. Zhao, Y. Li, Magnetron sputtering SiC films on nickel photonic crystals with high emissivity for high temperature applications, Appl. Surf. Sci. 259 (2012) 811–815.
[20] J.L. Xu, Z.C. Zhong, Z.X. Huang, J.M. Luo, Corrosion resistance of the titania particles enhanced acrylic resin composite coatings on sintered NdFeB permanent magnets, J. Alloy. Compd. 570 (2013) 28–33.
[21] S.D. Mao, H.X. Yang, J.L. Lin, H.G. Ying, Z.L. Song, The properties of aluminium coating on sintered NdFeB by DC magnetron sputtering, Vacuum 85 (2011) 772–775.
[22] J.L. Xu, Z.X. Huang, J.M. Luo, Z.C. Zhong, Corrosion behavior of sintered NdFeB magnets in different acidic solutions, Rare Met. Mater. Eng. 44 (2015) 786–790.
[23] H. Sepehri-Amin, Y. Une, T. Ohkubo, K. Hono, M. Sagawa, Microstructure of fine-grained Nd–Fe–B sintered magnets with high coercivity, Scr. Mater. 65 (2011) 396–399.
[24] K. Hono, H. Sepehri-Amin, Strategy for high-coercivity Nd–Fe–B magnets, Scr. Mater. 67 (2012) 530–535.